SPACE TELESCOPE SCIENCE INSTITUTE
Operated for NASA by AURA

Instrument Science Report COS 2012-02

Summary of the COS Cycle 17 Calibration Program

Rachel A. Osten[1], Michael Wolfe[1], Tom Ake[2], Alessandra Aloisi[1], K. Azalee Bostroem[1], William van Dyke Dixon[1], Parviz Ghavamian[1,3], Paul Goudfrooij[1], Justin Ely[1], Derck Massa[1], Sami-Matias Niemi[1,4], Cristina Oliveira[5,1], Steve Osterman[6], Ilaria Pascucci[1,7], Steve Penton[6,1], Charles Proffitt[2], David Sahnow[5,1], Tom Wheeler[1], Brian York[1], Wei Zheng[5]

[1] Space Telescope Science Institute, Baltimore, MD
[2] Space Telescope Science Institute/Computer Sciences Corporation, Baltimore, MD
[3] now at Towson University, Towson, MD
[4] now at Mulland Space Science Laboratory, United Kingdom
[5] Johns Hopkins University, Baltimore, MD
[6] CASA, University of Colorado, Boulder, CO
[7] now at University of Arizona, Tucson, AZ

November 29, 2012

ABSTRACT

We summarize the status of the calibration program for the Cosmic Origins Spectrograph during Cycle 17, which ran from August 2009 until October 2010.

Contents

1. Introduction

The Cosmic Origins Spectrograph (COS) was installed on the Hubble Space Telescope in May 2009. Cycle 17 was the first cycle of on-orbit operations of COS, following a period of on-orbit verification programs (Servicing Mission Observatory Verification 4, SMOV4). Cycle 17 observations commenced in August 2009 and ran through October 2010. The purpose of this document is to record and summarize the results of individual calibration programs. There were a few interruptions due to telescope safing events, which disrupted some of the regular monitoring programs. The Cycle 17 calibration program overlapped both Cycle 17 and 18 science programs. The timing of some SMOV programs ran into the nominal Cycle 17 time frame, which affected some Cycle 17 calibration programs which had overlapping functionality; consequently, the Cycle 17 programs were adjusted. The calibration program was set up before COS was installed on HST, and a supplemental calibration program was designed to expand upon initial on-orbit results. Section 2 gives a summary and overview of the calibration program, which comprises 18 unique programs, while section 3 details results from individual programs. The Appendix lists reference files and documentation produced as a result of Cycle 17 calibration programs.

2. Overview of Programs

Table 1 summarizes the orbit allocation and usage during the regular Cycle 17 calibration programs, as well as the supplemental programs. Table 2 provides a high level summary of the calibration programs, noting specifically products and accuracy achieved. The last column of Table 2 notes the page on which detailed information for that program can be found.

Table 1. Summary of orbit allocation and use during Cycle 17 COS calibration, including the supplemental calibration program.

	External		Internal	
	Regular	Supplemental	Regular	Supplemental
Allocated	111	39	457	5
Executed	107	38	401	5
Withdrawn	4	1	56	0
Failed	1	2	0	0
Repeated	1	0	0	0

ID	Proposal Title	Time Used (orbits) executed [allocated]		Products	Accuracy Achieved	Page
		External	Internal			
NUV Monitoring Programs						
11891	NUV MAMA Fold Distribution		1 [2]		<5% in location of peak of fold distribution	4
11894	NUV Detector Dark Monitor		114 [130]	cal. workshop paper‡, ISR, IHB & ETC update	0.2% in global dark rate uncertainty	7
11896	NUV Spectroscopic Sensitivity Monitor	41 [41]		cal. workshop paper‡, ref. file, ISR	min. SNR of 30 per resel at $\lambda_{\rm cen}$	9
11899	NUV Imaging Sensitivity	2 [2]		ISR	SNR of ≈ 60, observed to predicted count rates accuracy of ±0.01	12
11900	NUV Internal/External Wavelength Scale Monitor	14 [18]		–	7.2-15.5 pixels wavelength scale	15
FUV Monitoring Programs						
11895	FUV Detector Dark Monitor		286 [325]	ISR, cal. workshop paper‡, IHB & ETC update	0.1% in global dark rate uncertainty	16
11897	FUV Detector Sensitivity Monitor	46 [46]		cal. workshop paper‡, ISR, ref. file	SNR per resel of 30 at $\lambda_{\rm cen}$ for G140L, G130M; SNR∼23 for G160M	18
11997	FUV Internal/External Wavelength Scale Monitor	12 [12]		–	wavelength scale accuracy 5.7-7.5 pixels for G130M, 5.8-7.2 pixels for G160M, 7.5-12.5 pixels for G140L	20
Special Programs						
12010	COS FUV Line Spread Function Characterization	2 [2]		ISR, cal. workshop paper‡, tables of LSF models	SNR of 9.2 per resel in the continuum near 1530 Å	21
Supplemental Programs†						
12052	COS NUV Grating Efficiency Test		4 [4]	cal. workshop paper‡, ISR	few percent uncertainty in the ratio of count rates	23
12080	G140L Focus Sweep	5 [5]		ISR	30% uncertainty in autocorrelation FWHM of spectra	26
12081	COS Flux Calibration Below 1150 Å with G140L/1280	3 [3]		–	Poisson uncertainty over 20 pixels of 3% between 900–1150 Å, 10% between 300-700 Å	29
12082	Extending COS/G130M Coverage down to 905 Å with Two New Central Wavelengths	4 [5]		IHB update	wavelength scale: ±0.5 Å, sensitivity: ±5-10%, resolution: 20-30%	30
12083	G140L 1280 Wavecal Template		1 [1]	ref. file	N/A	31
12084	G140L 1280 Internal to External Wavelength Scales	1 [1]		ref. file	7.5-12.5 pixels wavelength scale accuracy	32
12085	STIS/E230M Data to Determine Internal to External Offsets in COS/G230L	1 [1]		–	unknown	33
12086	Generation of 1-D Fixed Pattern Templates	11 [11]		ref. file, ISR	2% Poisson uncertainty	34
12096	COS FUV Detector Lifetime Position Test	3 [3]		–	min. SNR per resel of 30 at $\lambda_{\rm cen}$	35

† Ten orbits were allocated (and executed) in the supplemental program 11897; these have been incorporated into the original program in this table.

‡ Proceedings of the calibration workshop can be found at `http://www.stsci.edu/institute/conference/cal10/proceedings`.

Table 2. Summary of Cycle 17 calibration and monitoring programs. Further details can be found in the following sections.

3. Results from Individual Programs

Proposal ID 11891: NUV MAMA Fold Distribution

Purpose and Description of Program

Proposal 11891, the NUV detector fold test, monitors the performance of the MAMA microchannel plate. The fold analysis provides a statistical measurement of the distribution of charge cloud sizes incident upon the anode giving some measure of changes in the pulse height distribution of the MCP and, therefore, MCP gain as charge is extracted from the microchannel plate.

A brief description of the steps involved is given here:

- Set the Software Global Monitor to a value that is large enough to permit a count rate spike when the lamp is turned on.
- Begin a 2300-second deuterium lamp exposure at MEDIUM current (lamp 2 is used) with OSM1 at the NCM1FLAT position, and OSM2 at G185M, with a central wavelength of 1850 Angstroms.
- During the exposure, enable each fold separately and collect counters X, Y, Z, W, VE, EV, and OR.

Execution

A one-orbit visit executed on May 4, 2010. A second visit was included in the program if the fold distribution is required more frequently than once a year, but it was withdrawn.

Summary of Analysis

The engineering telemetry data was examined (voltages, currents, temperatures, relay positions, status, and event counts) for agreement with predicted values and previous ground and on-orbit test data; all were nominal. The science exposure was used to construct a histogram of the number of counts for each fold. The results were compared and combined with the results from previous tests; all results were as expected. The combined results are shown below in Figure 1.

After the test, a dark exposure was taken where the counters were cycled. The post-analysis dark rate is plotted in Figure 2. There was a large increase in the dark count rate as each counter was sampled. This increase has been attributed to phosphorescence of the detectors window. Similar phosphorescence appears in the STIS NUV detector.

Accuracy Achieved	The position in the peak of the fold distribution was measured to better than 5% accuracy, in accordance with the Phase I goal.
Continuation Plans	This program was continued in Cycle 18 as Program 12419.

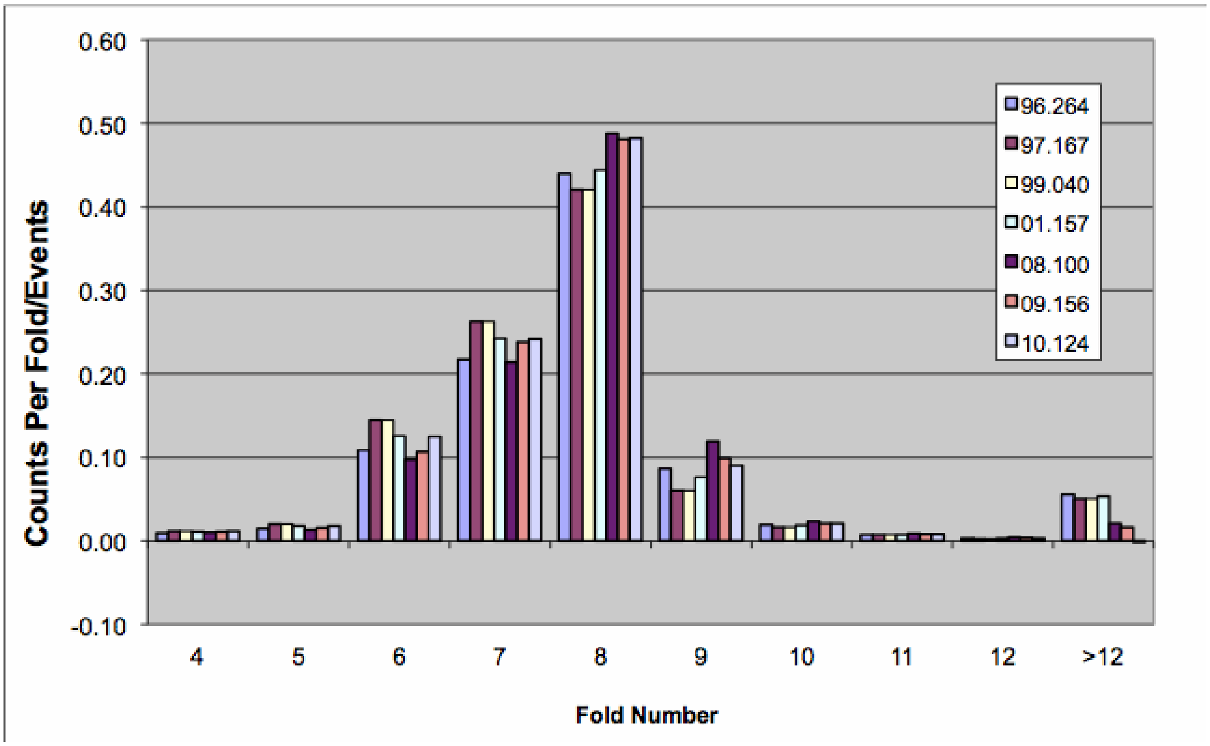

Figure 1. Histogram of COS NUV fold test results, including tests done on the ground. Legend gives the dates on which fold tests were performed, using the format “YY.DOY”; these include ground data.

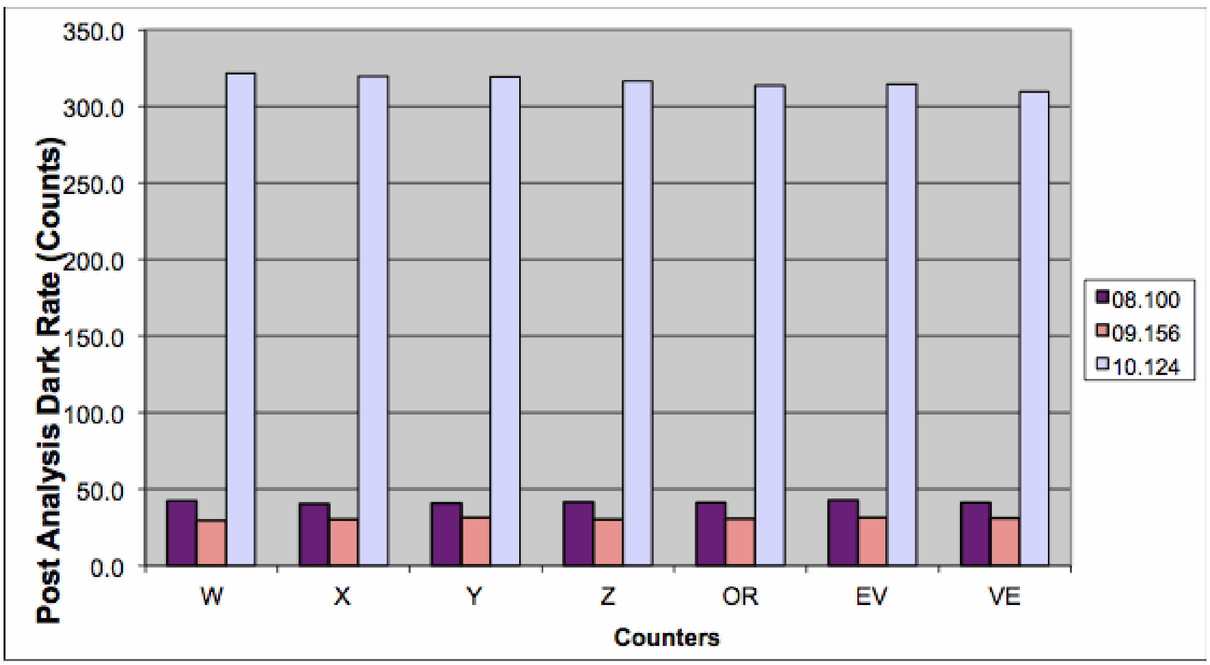

Figure 2. Post-test dark showing increased dark count rate. Legend is as in Figure 1. The original data (before 2008) do not contain any post-test dark count rate data.

Proposal ID 11894: NUV Detector Dark Monitor

Purpose and Description of Program	This proposal monitors the behavior of the dark current in the NUV MAMA detector. The spatial distribution of dark rate and the effect of the SAA were also studied.
Execution	Two exposures were taken weekly, to gain information about the dark rate as a function of MJD, passage through the SAA, and the detector temperature. The total number of exposures was 114. Sixteen visits were withdrawn because of telescope safing events.
Summary of Analysis	The NUV dark rate increases linearly and gradually over time (see Figure 3). Like its STIS counterpart, it also displays a dependence on the detector temperature. The COS dark rate is still considerably lower than that of STIS. Sahnow et al. (2011a) describe the analysis and results.
Accuracy Achieved	The Phase I accuracy requirement was a Poisson uncertainty of 1% for the global dark rate. The Poisson uncertainty in measurement of the global dark rate was 0.2%.
Continuation Plans	The program continued in Cycle 18 as 12420 with an observing frequency reduced to once per week.

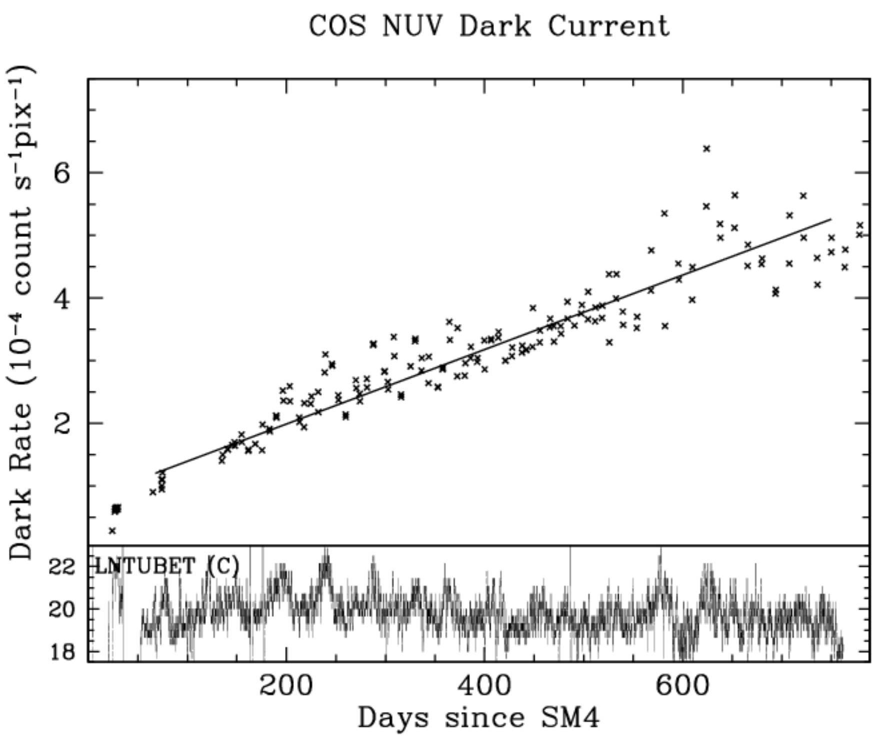

Figure 3. Top panel shows the COS NUV dark rate per pixel as a function of time. The bottom panel shows the temporal variation of the temperature. The line in the top panel is a fit to the temperature and time dependence of the dark rate, using an equation of the form $rate = \exp(A - B/(T + 273.16)) \times (1.5 + (MJD - 55097)/C) \times 10^{-4}$.

Proposal ID 11896: NUV Spectroscopic Sensitivity Monitor

Purpose and Description of Program The goal of the program was to monitor the time-dependent sensitivity so that corrections could be implemented to the pipeline flux calibration. Regular monitoring picks up any changes due to contamination or other sensitivity loss, and allows us to characterize these changes as a function of grating/wavelength.

Execution The program consists of monitoring observations of the NUV gratings, using external white dwarf spectrophotometric standard stars. The G230L gratings were monitored monthly, the G185M grating quarterly, and the G225M/G285M gratings monthly. A total of 41 orbits were used in this program. Visit AC had a guide star acquisition failure and was repeated by visit NC.

Summary of Analysis The time-dependent sensitivity was computed by taking ratios of net count rate spectra to the initial spectrum for a given configuration. The G230L and G185M gratings appeared to be relatively stable in time, showing no significant loss of sensitivity. However, the bare-Al gratings (G225M and G285M) exhibited sensitivity declines from the beginning of Cycle 17, which continue at a steady rate for each grating, being about -3.3 percent per year for G225M and -10.8 percent per year for G285M. These values are consistent with pre-launch trends done using grating efficiency tests. These values were implemented in a time-dependent sensitivity reference file, which was delivered to CDBS on July 14, 2010. A description of the analysis can be found in Osten et al. (2010).

During the course of investigating the spectroscopic sensitivity, it became apparent that the vignetting of the left edge of the NUV-MAMA detector described in Ake et al. (2010) was variable, producing changes of up to 10% of the relative sensitivity in this part of the detector. This variable vignetting was removed from the flat field reference files that had been delivered immediately after SMOV, and these were re-delivered to CDBS.

Accuracy Achieved The required accuracy for the program was a minimum S/N of 30 per resolution element at the central wavelength of each grating. This was achieved for all observations.

Continuation Plans	This program was continued in Cycle 18 as program ID 12421. Due to the low usage of the NUV gratings in GO observations, the monitoring frequency was dropped to quarterly in Cycle 18.

Proposal ID 11899: NUV Imaging Sensitivity

Purpose and Description of Program

The goal of the program was to test the NUV imaging sensitivity, by observing stars with a range of colors, and placing the same star at different positions in the aperture.

Execution

There were no anomalies with the program execution.

Summary of Analysis

Targets with an appropriate range of colors were observed to establish color terms in the sensitivity formula. A total of ten horizontal branch stars in the globular cluster NGC6681 were observed. STIS spectra of all the stars exist, and these spectra plus an extension from 5700 Å to 10000 Å using Castelli-Kurucz models were used as input to Pysynphot to generate the predicted count rates. The observed count rate of each star was measured using aperture photometry, through an encircled energy curve to extrapolate the measured flux to an infinite aperture. Stellar temperatures were derived by fitting the STIS spectra to Castelli & Kurucz models with the cluster metallicity and reddening. Preliminary results are shown in Figure 4, and show a systematic offset of 5-10% below unity, with a color-dependent trend. The temperature dependence is likely a combined effect of the need for an updated throughput curve and detector sensitivity.
In addition, the solar-type star P177D was used to test the throughput of MIRRORB as a function of position in the aperture, using nine locations within the PSA with a step size of 0.25 arcsec. The throughput did not apparently peak in the center of the aperture (see Figure 5). The regions used to perform the photometry were defined so that they excluded the fainter of the two images generated from MIRRORB, being 15 pixels in radius for the source, and a sky annulus extending from 25–35 pixels from the source. The secondary images lies 20 pixels from the primary, so it did not contribute to either the star or the sky measurements. The faintest exposure was #6 and the brightest #9, differing by 5σ, with a general trend of increasing brightness from left to right.

An ISR (Bostroem et al.) describing the analysis and results further is in preparation.

Accuracy Achieved The SNR using counting statistics of the measurements of the solar-type star is ≈ 60. The observed to predicted count rates of the globular cluster stars had an accuracy of ± 0.01.

Continuation Plans This program was not continued in Cycle 18.

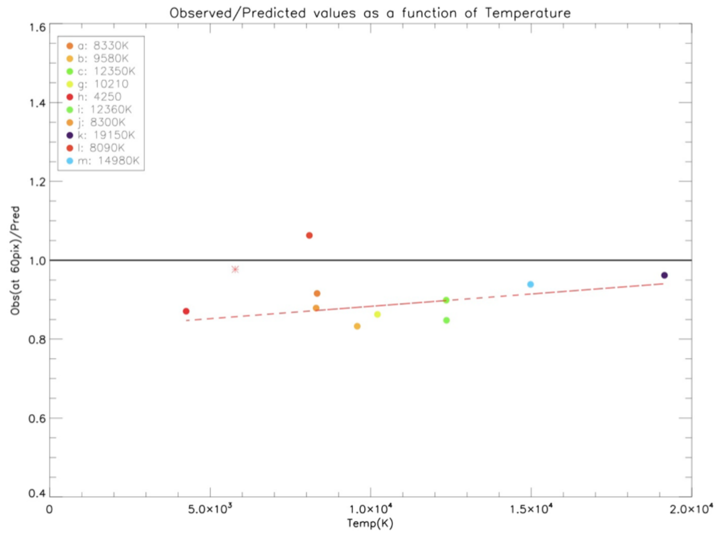

Figure 4. Ratio of observed to predicted count rate for 10 stars in the globular cluster NGC 6681 as a function of stellar effective temperature. The solid horizontal line indicates a ratio of unity. The dashed line is a linear fit to the trend of ratios versus stellar effective temperature.

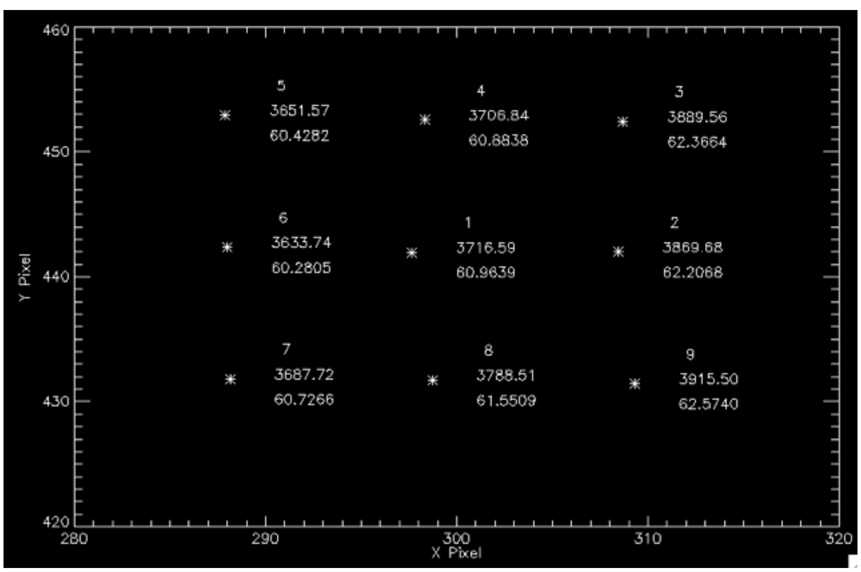

Figure 5. Plot of throughput of a solar-type star as a function of position in the aperture, using the PSA and MIRRORB. Asterisks represent the stellar centroids. The three numbers by each asterisk give the exposure number, the total counts in the star, and the square root of the counts, respectively.

Proposal ID 11900: NUV Internal/External Wavelength Scale Monitor

Purpose and Description of Program

This program monitored periodically ($\sim$ every 2-3 months) the offsets between the wavelength scale set by the internal wavecal versus that defined by absorption lines in external targets. This was accomplished by observing two external radial velocity standard targets: HD187691 with G225M and G285M and HD6655 with G285M and G230L. The two standard targets have little flux in the wavelength range covered by G185M and so Feige 48 (sdO) was supposed to be observed with this grating. After this program was put in place and some of the Feige 48 visits were executed it was decided that this target was not suitable to monitor the wavelength offsets. A new target has not been identified, due to the difficulty of finding an adequate replacement, the low priority of this mode, and the low usage of this mode in Cycle 18.

Execution

14 out of 18 planned visits of this program were executed. Visit 04 was withdrawn because the end of SMOV was delayed from when this program was put together and this visit was no longer needed. Visits 12, 13, and 14 were withdrawn because, unknown to us when this program was crafted, the target in these visits (Feige 48) was not the most suitable for the objectives of the program — it is a member of a binary system, and is a pulsating subdwarf O star. All the visits that executed had no issues.

Summary of Analysis

Due to the low GO usage of the NUV modes, the priority of the NUV wavelength monitoring analysis was lowered and the analysis has not been completed yet.

Accuracy Achieved

At this point the accuracy achieved is not known.

Continuation Plans

A program similar to this in design was carried out in Cycle 18 as program 12422, with a reduced observing frequency.

Proposal ID 11895: FUV Detector Dark Monitor

Purpose and Description of Program	This program monitored the behavior of the dark current of the FUV detector on a weekly basis.
Execution	Although 325 orbits were allocated, 287 were executed, 35 were withdrawn, and 3 had some data loss. The visits were organized in groups of five occurring every week. Each exposure lasted 1330 seconds.
Summary of Analysis	The dark rate remained at a low and stable level (see Figure 6); it is dependent on proximity to the SAA as well as detector temperature. An ISR (Sahnow et al. 2011b) has been published describing the analysis and results in more detail. At a level of 3.5×10^{-6} count/sec/pixel, the dark rate is within anticipated values.
Accuracy Achieved	The Phase I accuracy requirements for this program were to obtain a few counts per exposure, and build up decent S/N over time. The Poisson uncertainty in the global dark rate for each exposure, over the active area, is $<0.1\%$. Summing up the dark rate over all 286 dark exposures, the S/N per pixel is ~ 1.
Continuation Plans	The program continued in Cycle 18 as 12423 with an observing frequency reduced from weekly to bi-weekly groups of five visits.

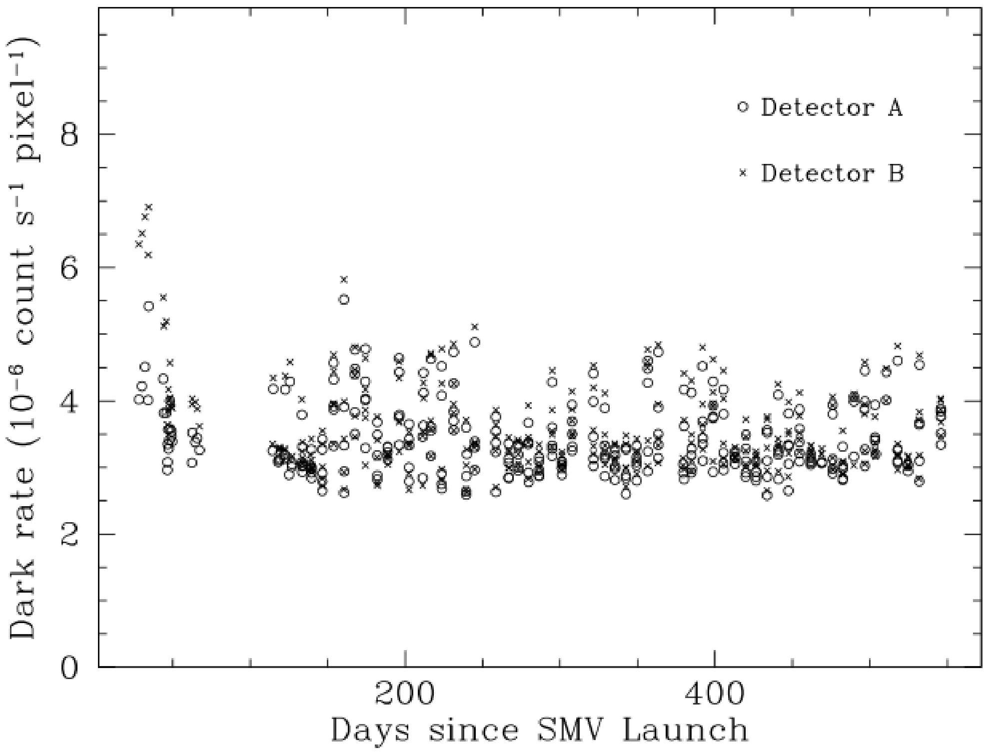

Figure 6. FUV dark rate as a function of time.

Proposal ID 11897: FUV Detector Sensitivity Monitor

Purpose and Description of Program

The goal of the program was to monitor the sensitivity of each FUV grating mode using external white dwarf spectrophotometric standard stars to detect and characterize any changes.

Execution

No problems were encountered in executing the program. The program consisted initially of monthly monitoring of the G140L grating, and quarterly monitoring of the G130M and G160M gratings. After the first 4 months, it became apparent that the FUV detector was experiencing a marked sensitivity loss, and the monitoring frequency was increased to monthly for all FUV gratings in the supplemental program. A total of 46 orbits were used.

Summary of Analysis

During the first several months of on-orbit operations of the COS FUV detector, it became apparent that the spectroscopic sensitivity was changing with time at a rate larger than previously anticipated. The sensitivity decline was affecting all FUV gratings, with an increase in degradation at the longest FUV wavelengths. The initial results of this monitoring were described in Osten et al. (2010), and resulted in the delivery of a time-dependent sensitivity (TDS) reference file on July 14, 2010 for use in the flux calibration of spectroscopic data. Regular monitoring of spectrophotometric white dwarf standard stars continues, and has revealed a change in the rate at which the sensitivity decline is occurring, as well as its behavior with wavelength. The new trends show that around mid-March 2010, the rate of sensitivity decline slowed markedly and became nearly wavelength independent. From mid-March 2010 until the end of Cycle 17, the rate of sensitivity decline has been much more consistent across the FUV gratings and detector segments, with a nearly grey wavelength dependence.

A new FUV TDS reference files was delivered on March 18, 2011 to the calibration database system for use with COS/FUV. These files are now routinely used in on-the-fly-reprocessing of COS data obtained through the archive. These files should correct fluxes to an accuracy of +/-2% for data taken in the period overlapping the sensitivity monitor program. The updated results of the spectroscopic sensitivity monitoring are described in an ISR (Osten et al. 2011).

Accuracy Achieved The Phase I accuracy requirement was a SNR (per resel) of 30 at the central wavelength. This accuracy was achieved for G140L and G130M, and the G160M observations had a SNR per resel at the central wavelength of about 23.

Continuation Plans This program was continued in Cycle 18, with program ID 12424.

Proposal ID 11997: FUV Internal/External Wavelength Monitor

Purpose and Description of Program	This program monitored periodically the offsets between the wavelength scale set by the internal wavecal versus that defined by absorption lines in external targets (each target is observed once every 2–3 months). This is accomplished by observing two external targets in the SMC: SK191 with G130M and G160M and Cl* NGC 330 ROB B37 with G140L (SK191 is too bright to be observed with G140L).
Execution	This program observed 2 external targets every 2-3 months for a total of 12 visits (1 orbit each). Visit 09 failed because the FGS failed to acquire the guide stars.
Summary of Analysis	Analysis of this program consisted in determining the centroids of several absorption lines spread throughout the COS spectrum and then comparing them to the centroids derived for the same lines in the STIS data and also tracking how the centroids of COS lines changed over different visits.
Accuracy Achieved	The accuracy achieved of the wavelength scale is 5.7-7.5 pixels for G130M, 5.8-7.2 pixels for G160M, and 7.5-12.5 pixels for G140L. This is $\approx$ one resel for the M modes, and $\approx$ 2 resels for the G140L grating (one resel is 6 pixels).
Continuation Plans	This program was continued in Cycle 18, with less frequency, as program 12425.

Proposal ID 12010: COS FUV Line Spread Function Characterization

Purpose and Description of Program

In this program E140H STIS spectra were acquired of the O9b star Sk-155 (0.2x0.09 aperture, CENWAVE=1598 A) in order to create a high resolution spectrum covering the wavelength range of COS G160M . Matching E140H spectra covering the COS G130M spectral range already existed from a Cycle 10 GO program. The goal was to test the validity of the COS line spread function (LSF) models by convolving the E140H spectra with model LSFs and comparing these to the COS G130M and G160M spectra.

Execution

No anomalies were encountered in executing this program.

Summary of Analysis

The STIS E140H spectra were convolved with the COS LSF models described in Ghavamian et al. (2009). The models included the mid-frequency wavefront errors introduced by polishing errors on the COS OTA. These convolved spectra were compared to the G130M and G160M spectra, along with STIS E140H spectra that had been convolved with a Gaussian LSF (representative of the LSF from thermal vacuum tests) at the intended spectral resolution of COS ($\sim$20,000).

The results of the analysis were that the STIS spectra convolved with the COS LSF including the mid-frequency wave front errors (MFWFEs) were significantly superior to those where STIS spectra had been convolved with a simple Gaussian. The redistribution of flux from the cores of the LSFs into the wings were needed to reproduce such features as the residual fluxes observed in the cores of saturated absorption lines, as well as the blending of close together spectral lines and the disappearance of some of the weak, narrow absorption lines seen in the unconvolved E140H spectra.

An ISR (Ghavamian et al. 2009) details the full analysis and results of this program.

Accuracy Achieved The spectra convolved with the COS LSF compare well with what was expected, though since publication of the ISR in 2009 it has been proposed that an additional 3% of the flux from the core of the LSF is distributed out to the wings due to micro-roughness on the HST OTA mirrors (Kriss et al. 2011). The data from this program were also used in that analysis. The exposure time was set to achieve a S/N of 10 in the continuum near 1530 Å, and the S/N obtained was 9.2.

Continuation Plans This program was not continued in Cycle 18, as the LSF properties have now been characterized and are not expected to change with time.

Proposal ID 12052: COS NUV Grating Efficiency Test

Purpose and Description of Program

The goal of the program was to perform two more grating efficiency tests (in addition to the one performed in SMOV) to enable better comparison of results of grating efficiency tests done on the ground with external target spectroscopic sensitivity monitoring on orbit.

Execution

The program executed without any incident. There were two visits, for a total of 4 internal orbits.

Summary of Analysis

The grating efficiency test (GET) contains 10 NUV exposures designed to obtain the same S/N of various emission lines throughout the NUV band. The sequence and duration of exposures in this NUV GET are the same as used by the IDT on the ground from 2004-2009 to monitor the relative efficiencies of the NUV gratings. The sequence starts with a 20-minute wait, to ensure that the lamp has cooled from any usage in a previous visit. Analysis of the results of the first test is described in an ISR, Osten et al. (2010). Analysis of the second visit, which occurred in August 2010, was done in the same way. The results show that the trends seen on the ground, indicating an efficiency decline in the G225M and G285M gratings relative to the G230L grating, continue to apply in orbit. The loss in efficiency seen in external targets is thus apparently a continuation of the trends first noticed on the ground. Figures 7 and 8 give graphical displays of the results, while Table 3 lists the slopes derived from both ground-based data and on-orbit data.

Accuracy Achieved

The accuracy achieved was a few percent in the ratio of count rates.

Continuation Plans

Because this program demonstrated that there is no additional sensitivity losses encountered in the G225M and G285M gratings on orbit compared to what was seen on the ground, it was decided that the spectroscopic sensitivity monitor using external white dwarf spectrophotometric standard stars would be continued and this program discontinued.

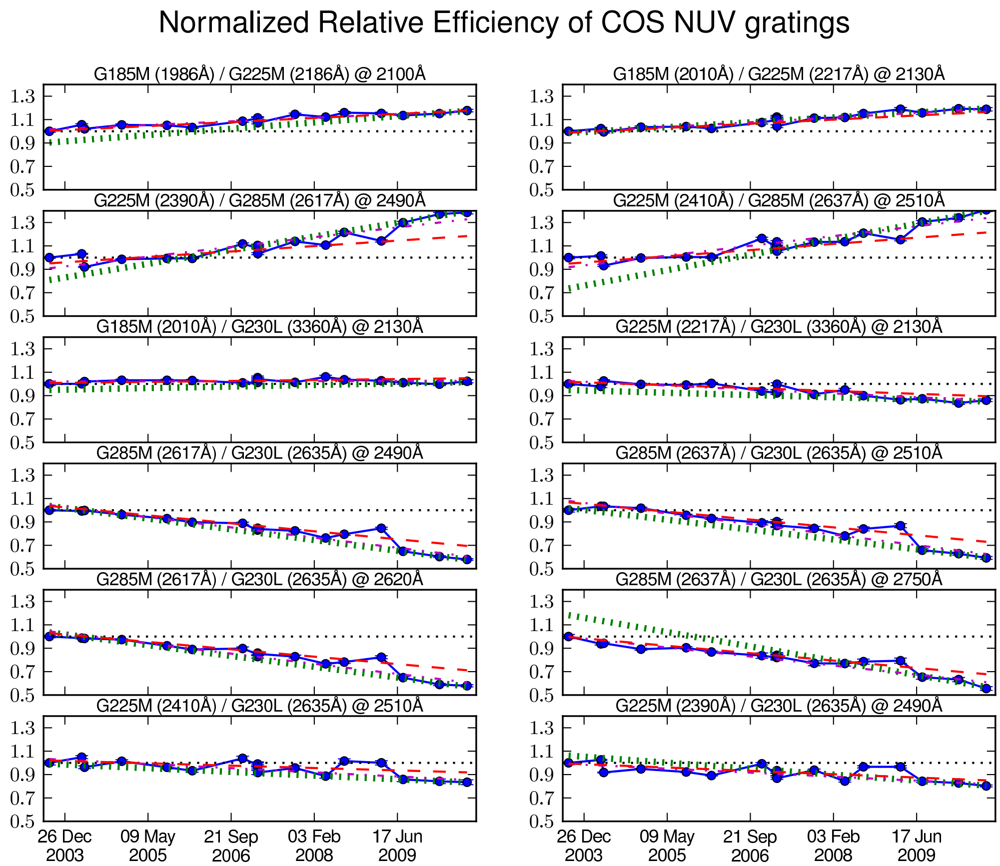

Figure 7. Temporal dependence of the normalized relative efficiency of the COS NUV gratings. All but the last 3 data points were obtained on the ground; the last 3 data points were obtained on orbit. The last two points before launch show up as outliers on several plots and were removed from fitting reported in Table 3. The outlier measurements were made in late 2008/early 2009 while COS was at the Kennedy Space Center, and may have been affected by the increase in humidity at Cape Canaveral. The conditions during these two GETs may thus have been different from the other ground tests. The gratings and central wavelengths used to perform the ratio, as well as the wavelength at which the ratio is taken, are indicated in the title of each sub-plot.

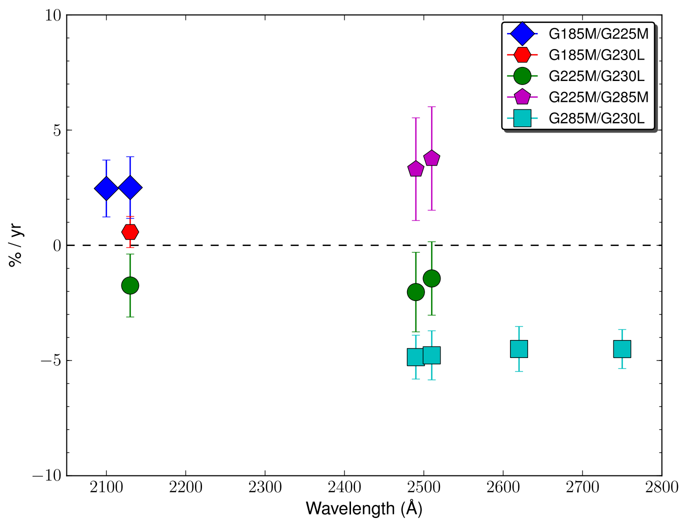

Figure 8. Summary of NUV GET results by wavelength.

Table 3. Summary of NUV GET results

wavelength (Å)	grating pair (grating$_1$($\lambda_{cen,1}$)/grating$_2$/($\lambda_{cen,2}$))	all data (exclud. outliers) (%/year)	on-orbit data (%/year)
2100	G185M(1986)/G225M(2186)	2.2±0.5	3.8±1.5
2130	G185M (2010)/G230L(3360)	0.1±0.5	0.9±4.2
2130	G225M(2217)/G230L(3360)	-2.4±0.6	-1.4±6.3
2130	G185M(2010)/G225M(2217)	2.8±0.5	3.0±3.8
2490	G225M(2390)/G230L(2635)	-2.4±0.9	-3.6±1.6
2490	G285M(2617)/G230L(2635)	-6.2±0.6	-6.5±1.2
2490	G225M(2390)/G285M(2617)	5.9±1.4	8.3±5
2510	G225M(2410)/G230L(2635)	-2.5±1.0	-2.2±0.5
2510	G285M(2637)/G230L(2635)	-6.4±0.8	-6.0±1.7
2510	G225M(2410)/G285M(2637)	5.9±1.3	9.4±5.1
2620	G285M(2617)/G230L(2635)	-6.2±0.8	-6.6±4.4
2750	G285M(2637)/G230L(2635)	-5.5±0.7	-8.7±7.4

Proposal ID 12080: G140L Focus Sweep

Purpose and Description of Program	The goal was to determine the optimum focus setting for the COS FUV channel to within 200 focus steps for the G140L grating.
Execution	The program executed as designed, in one visit.
Summary of Analysis	The focus sweep consisted of a series of 17 G140L spectra of the B2Ia star Azv18, taken at the 1105 A CENWAVE and FPPOS (=3) settings. The sweep was performed in increments of 100 focus steps, running from focus offsets of -800 to +800 relative to the nominal focus. After minimizing the impact of grid wire shadows in the spectra (via usage of a gridwire flat) and correcting the focus values for effects of on-orbit breathing of the HST OTA, the spectra taken at the different focus settings were compared to one another to locate the focus setting with the narrowest, sharpest absorption lines. The full width half maximum of the autocorrelation function was determined for each of the spectra, with the expectation that the autocorrelation widths would follow a roughly quadratic variation curve with focus setting. The focus curve showed a very shallow, broad minimum (see Figure 9). Fitting the inner points of the focus curve with a quadratic function, the minimum (i.e, optimum focus) was found to occur at a focus offset of -415 steps from the nominal absolute focus value of -370 steps. However, this result is not firm enough to justify moving the G140L focus by this amount, because the error bars in the autocorrelation FWHM are large enough to overlap between all the fitted datapoints. In addition, direct visual inspection of spectra taken near the derived optimum focus and those taken at nominal focus do not show marked differences in the widths or sharpness of the lines. The bottom line is that there is no compelling reason to move the nominal focus of G140L from its current location. An ISR (Ghavamian et al. 2012) documents the analysis summarized above.

Accuracy Achieved The shallowness of the focus curve derived from the observations along with the significant uncertainty in the autocorrelation FWHM of the spectra ($\sim 30\%$) prevents the determination of the optimum focus to within the desired 200 focus steps.

Continuation Plans The program was not continued - the lack of a firm value for the optimum G140L focus setting is not a result which will be improved upon or is expected to change in future cycles.

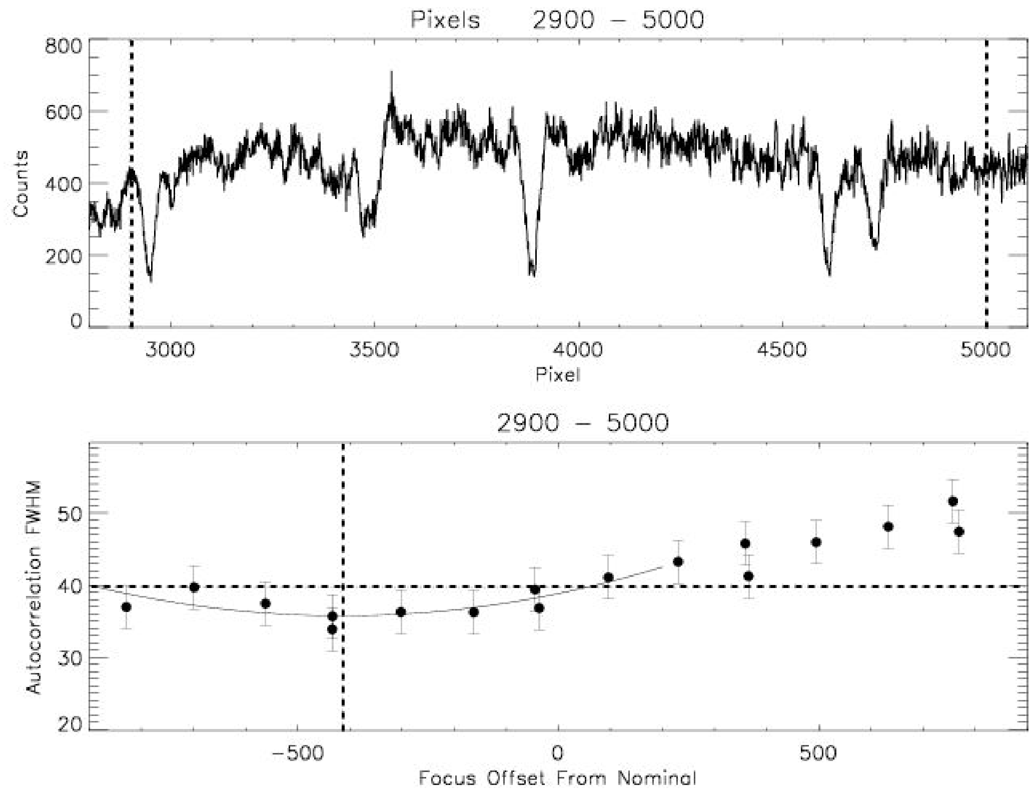

Figure 9. Top panel shows a section of the G140L spectrum used to perform focus measurements – the spectrum between the two vertical dashed lines was used. Bottom panel shows the focus curve – the autocorrelation as a function of focus offset from nominal. The vertical dashed line indicates the location of the minimum in the focus curve, and the horizontal dashed line indicates an amount which is $\approx 1\sigma$ away from the minimum of the curve. The autocorrelation FWHM of all of the points with less than zero focus offset from nominal lie within this range, demonstrating the uncertainty of the final result.

Proposal ID 12081: COS Flux Calibration Below 1150 Å with G140L/1280

Purpose and Description of Program

The goal of this program was to establish a flux calibration for the new G140L/1280 cenwave setting concentrating on the short wavelength segment on FUVB. McCandliss et al. (2010) demonstrated that the G140L Segment B channel does indeed have FUV sensitivity. When the original SMOV flux calibration program was devised, it was not clear whether there would be any sensitivity below 1150 Å, and the target used for the initial flux calibration (described in Massa et al. 2010) was not bright enough at these wavelengths for an accurate flux calibration. The program was also intended to determine whether COS has any sensitivity to EUV radiation (below 700 Å).

Execution

There were no anomalies in the execution of the program.

Summary of Analysis

The data were obtained, a new model for the target (GD 50) was provided, and an initial calibration was performed. It was also determined that there is some EUV response, but exactly how much depends upon an uncertain wavelength scale. There are no wavelength calibration lines falling on segment B in this configuration, and for safety reasons segment A was turned off. The pipeline needs to be modified to handle the lack of wavecal lines, and this has been deemed a lower priority effort. The flux calibration analysis has been postponed because of these wavelength calibration issues. Spectra taken at different FP-POS positions were manually shifted and added. There is a little EUV sensitivity (<1 cm^2), but it appears to drop below zero around 500 Å. Data were obtained at all 4 FPPOS positions, so the same data will be used to determine the fixed pattern noise in the G140L grating.

Accuracy Achieved

The accuracy achieved was a Poisson uncertainty of 3% over the range 900–1150 Å, and 10% over the range 300-700 Å.

Continuation Plans

This program was not continued in Cycle 18, since there is no reason to repeat it until there is a major change in the instrumental configuration, e.g., changing to a new lifetime position.

Proposal ID 12082: Extending COS/G130M Coverage Down to 905 Å with Two New Central Wavelengths

Purpose and Description of Program	The goals of this program were to explore the possibility of using the G130M grating at a position to cover the spectral region between the low wavelength cutoff of the G130M/1291 setting and the HST/COS cutoff near 905 Å. Specifically, the wavebands, sensitivity, and resolution were to be determined for these two central wavelengths.
Execution	There were no problems in executing the proposal. The program consisted of 3 visits which occurred on June 1, July 27, and August 10, 2010. The first visit was an exploratory one, testing two central wavelengths covering 905-1208 Å (G130M/1066) and 1021-1324 Å (G130M/1184). After analyzing the sensitivity curves, these wavebands were adjusted to 900-1041 Å (Segment B) and 1055-1096 Å (Segment A) and 940-11081 Å (Segment A) and 1096-1238 Å (Segment B). These central wavelength settings are known as G130M/1055 and G160M/1096, respectively.
Summary of Analysis	The wavebands and sensitivity curves for the new central wavelengths were reasonably well determined. The resolution was not as well determined due to the target being significantly out of focus, and the limited number of unblended lines/absorption features in the targets observed. These results were presented in Osterman et al. (2010) and Penton et al. (2011). The analysis was used to prepare a section of the Cycle 19 call for proposals, and COS Instrument Handbook.
Accuracy Achieved	Wavelength scale: ±0.5Å (zero point) Sensitivity : ±5-10% Resolution : 20-30% These sensitivity and resolution accuracies are for the initial focus values, which were not optimized for this setting. Subsequent updates to the focus values have improved the spectral resolution and sensitivity significantly.
Continuation Plans	These modes have been offered to proposers as of Cycle 19. Additional calibrations, and flight and ground software modifications, have been performed in Cycle 19 program 13070, making these supported modes.

Proposal ID 12083: G140L/1280 Wavecal Template

Purpose and Description of Program	This internal only program had the goal of obtaining lamp template spectra with the G140L grating at all FPPOS, using the 1280 cenwave which only started to be available to users in Cycle 18. This G140L/1280 central wavelength replaces the original 1230 central wavelength, as it was discovered during SMOV that the G140L/1230 central wavelength places zeroth order light on the detector at FP-POS=4.
Execution	This internal program was executed once, in 1 visit in September 2010. There were no issues in obtaining the data.
Summary of Analysis	Data was analyzed by extracting 1d-spectra from thermal and geometrically corrected data. To determine if OSM mechanism drift was present, data was split into short $\sim$20 sec exposures, each short exposure was cross-correlated with the first short exposure. No drift was present. Data was used to update lamp template reference file and the file v3g18195l_lamp.fits was delivered to CDBS.
Accuracy Achieved	N/A
Continuation Plans	This program was not repeated in Cycle 18 as this was a one time program to provide a template for a mode not previously available that replaces an older one.

Proposal ID 12084:G140L/1280 Internal to External Wavelength Scales

Purpose and Description of Program

This program observed NGC330-B37 to determine the offsets between the PSA and WCA wavelength scales (for FP-POS=3) for the G140L/1280 mode which replaced the G140L/1230 central wavelength in Cycle 18.

Execution

This program consisted of 1 visit that observed an external target. There were no issues with the observations.

Summary of Analysis

The analysis of the data is similar to that described in Oliveira et al. (2010). In summary, these data were partially calibrated with the COS pipeline and then, in conjunction with STIS data of the same target, used to derive offsets between the PSA and WCA wavelength scales. The offsets derived in the analysis were used to update the wavelength dispersion reference file, v3g18194l_disp.fits, which was delivered to CDBS.

Accuracy Achieved

The accuracy achieved is 7.5–12.5 pixels, which is consistent with the requirements, and with what was expected at the phase I level.

Continuation Plans

This program was not continued in Cycle 18 as this was a one time program to calibrate a mode not previously available. However, a program in Cycle 18 (12425) monitors this new mode that replaces G140L/1230.

Proposal ID 12085: STIS/E230M Data to Determine Internal to External Offsets in COS/G230L

Purpose and Description of Program	This program observed HD 6655, a radial velocity target that is used for calibrating COS/G230L. The objective of this program was to obtain STIS data of this target with the E230M grating, and then to use these observations to derive the offsets between the internal and external COS/G230L wavelength scales. COS/G230L data of this target was obtained during SMOV, the STIS data was needed as a reference for the COS wavelengths.
Execution	This external program was executed once, in 1 visit in July 2010. There were no issues in obtaining the data
Summary of Analysis	Due to the low GO usage of the NUV modes, the priority of the NUV wavelength scales was lowered and the analysis has not been completed yet.
Accuracy Achieved	At this point this is unknown.
Continuation Plans	This program was not continued in Cycle 18 as this was a one time observation to obtain STIS data to support COS calibrations.

Proposal ID 12086: Generation of 1-D Fixed Pattern Templates

Purpose and Description of Program
The goals of this proposal were to supplement high S/N data obtained in SMOV at the middle CENWAVE (in program 11494) with similar data at the extreme CENWAVEs. These data were to be used to generate 1-D fixed pattern noise templates.

Execution
The program executed as planned; there were no issues.

Summary of Analysis
Along with the main goal, the same data revealed several unexpected effects. Specifically:

1. Comparison between the SMOV and 12086 data revealed the presence of gain sag in the response, which showed itself as changes in fixed pattern noise.

2. The availability of high S/N data at more than one CENWAVE revealed that the instrumental response was CENWAVE dependent at the +/-5% level. This includes large scale variations and a specific feature in the G130M that appears near 1180 Å, but varies with CENWAVE.

3. These data were combined with earlier data to produce the grid wire template which was delivered for the G130M and G160M gratings. It is also being used in the ongoing effort to produce a full 1D-flat. Ely et al. (2011) describe the generation of COS FUV gridwire flat-field templates.

Accuracy Achieved
2% Poisson accuracy

Continuation Plans
The current program instigated a Cycle 18 program to fully calibrate all of the CENWAVEs with high S/N data obtained simultaneously (Program 12426).

Proposal ID 12096: COS FUV Detector Lifetime Position Test

Purpose and Description of Program	To measure the properties of the COS FUV detector at several lifetime positions (offsets of -6.0, -3.0, +1.2, +3.0, +6.0 arcseconds) for all three gratings, and to determine if the time dependent sensitivity was due to detector illumination.
Execution	The detector shut down due to light from the wavecal lamp leaking through the FCA at an offset position of +6.0". As a result, we only collected the expected data at offset positions +1.2" and +3.0" using G140L.
Summary of Analysis	The data verified that the loss of throughput as a function of time was not due to the number of photons collected by the detector, but rather that the sensitivity loss was due to global photo-cathode degeneration (Proffitt et al. in preparation). This program, along with others, did highlight the effect of the gain sag. A presentation was made to GSFC about the shutdown (22 March 2010), and a short memo was written (Sensitivity vs. Cumulative Detector Exposure, 29 March 2010).
Accuracy Achieved	The program was designed to be compared to data taken from the FUV sensitivity monitoring program, and for the exposures which did not trip the global count rate limit, a similar accuracy was achieved, namely, minimum SNR of 30 per resel near the central wavelength of the grating.
Continuation Plans	There were no plans to continue this program, as it demonstrated the non-localized nature of the sensitivity degradation. Programs 12676, 12677, and 12678 were carried out during Cycle 18 to determine the detector properties over the active area. The analysis of these programs allowed us to develop a strategy to move to a difference lifetime position in order to mitigate gain sag effects.

Acknowledgments

Change History for COS ISR 2011-01

Version 1: November 29, 2012- Original Document

References

Ake, T. et al. 2010, COS Instrument Science Report 2010-03
Ely, J. et al. 2011, COS Instrument Science Report 2011-03
Ghavamian, P. et al. 2009, COS Instrument Science Report 2009-01
Ghavamian, P. et al. 2012, COS Instrument Science Report, 2012-01
Kriss, G. et al. 2011, COS Instrument Science Report, 2011-01
Massa, D. et al., 2010, COS Instrument Science Report 2010-02
McCandliss, S. R. et al. 2010 ApJ 709, L183
Oliveira, C. et al. 2010, COS Instrument Science Report 2010-06
Osten, R. et al. 2010, COS Instrument Science Report 2010-15
Osten, R. et al. 2011, COS Instrument Science Report 2011-03
Osterman, S. et al. 2010, STScI Calibration Workshop
Penton, S. et al. 2011 BAAS 217, 25428
Proffitt, C. et al. 2012, COS Instrument Science Report, in preparation
Sahnow et al. 2011a COS Instrument Science Report 2010-12
Sahnow, et al. 2011b COS Instrument Science Report 2010-11

Appendix

Table 4 lists the COS reference files delivered as part of analysis of data taken in COS Cycle 17 calibration programs. Table 5 lists the instrument science reports and technical instrument reports produced as a result of analysis of Cycle 17 calibration programs. Table 6 lists the contributions to the 2010 STScI Calibration Workshop based on COS Cycle 17 programs.

Table 4. COS Cycle 17 Reference File Deliveries

Reference File	File type	Delivery Date	Contributing Programs
NUV Reference Files			
NUV flat field	*flat.fits	Feb. 14, 2011	11896
NUV Time-Dependent Sensitivity	*tds.fits	July 13, 2010	11896
FUV Reference Files			
FUV wave. disp. solutions	*disp.fits	March 26, 2011	12083,12084
FUV flat field	*flat.fits	April 7, 2011 April 28, 2011	11491, 11497, 11897
FUV sensitivity	*phot.fits	Aug. 20, 2010	12081
FUV lamp template	*lamp.fits	March 16, 2011	12083
FUV data quality	*bpix.fits	March 10, 2010	11491, 11895
FUV pulse-height parameters	*pha.fits	Jan. 29, 2010 Dec. 21, 2010	11482, 11895 11895, 11897
FUV Time-Dependent Sensitivity	*tds.fits	July 13, 2010 March 18, 2011	11897 11897, 12424

Table 5. Instrument Science Reports & Technical Instrument Reports Produced from Cycle 17 Calibration Programs

Number	Contributing Programs	First Author	Title
ISR2009-01	12010	P. Ghavamian	Preliminary Characterization of the Post-Launch Line Spread Function of COS
ISR2010-11	11482, 11895	Sahnow	COS FUV Detector Dark Rates during SMOV and Cycle 17
ISR2010-12	11466, 11894	Sahnow	COS NUV Detector Dark Rates during SMOV and Cycle 17
ISR2010-15	11896, 11897, 12052	R. A. Osten	Early Results from the COS Spectroscopic Sensitivity Monitoring Programs
ISR2011-01	12010	G. Kriss	Improved Medium Resolution Line Spread Function for the COS FUV Spectrum
ISR2011-02	11897, 12424	R. A. Osten	Updated Results from the COS Spectroscopic Sensitivity Monitoring Program
ISR2011-03	12086	J. Ely	COS FUV Gridwire Flat Field Template
ISR2012-01	12080	P. Ghavamian	COS FUV Focus Determination for the G140L Grating
in prep.	11899	K. Bostroem	COS NUV Imaging Sensitivity Calibration

Table 6. Contributions to the 2010 STScI Calibration Workshop Based on COS Cycle 17 Programs[1].

First Author	Type	Title
Ake, T.	Talk	COS FUV Flat Fields and Signal to Noise Characteristics
Aloisi, A.	Talk	The On-Orbit Performance of the Cosmic Origins Spectrograph
Osten, R.	Talk	COS Sensitivity Trends in Cycle 17
Osterman, S.	Talk	Observing with HST below 1150 Å: Extending COS/G130M and G140L coverage to 905 Å
Ghavamian, P.	Poster	COS External Spectroscopic Performance: FUV Spectral and Spatial Resolution
Oliveira, C.	Poster	Wavelength Calibration of the Cosmic Origins Spectrograph
Pascucci, I.	Poster	Monitoring of the Wavelength Calibration Lamps for the Hubble Space Telescope
Penton, S.	Poster	On-Orbit Performance of the COS Target Acquisitions
Sahnow, D.	Poster	On-Orbit Performance of the COS Detectors
Zheng, W.	Poster	Trend of Dark Rates of the COS and STIS MAMA Detectors

[1] Proceedings of the calibration workshop can be found at `http://www.stsci.edu./institute/conference/cal10/proceedings`.